can occur. The early expectations that the lanthanides would have little chemistry with unsaturated hydrocarbons were based on too limited a set of complexes. The prediction[9] that the lanthanides would have a much broader coordination chemistry if the metals were placed in the proper oxidation state and coordination environment is continually being substantiated. The $(C_5Me_5)_2Sm$ moiety appears to be one unit which has the necessary characteristics to achieve significant interactions with a broad range of substrates. The μ-η^2:η^2-bimetallic coordination mode of $(C_5Me_5)_2Sm$ to stilbene, styrene, and dinitrogen[7] may be general for unsaturated ligands, although in many cases any initially formed $[(C_5Me_5)_2Sm]_2$(unsaturated ligand) complex may be too reactive to isolate. The chemical consequences of the μ-η^2:η^2-alkene and η^2-arene lanthanide coordination modes are under study.

Acknowledgment. We thank the National Science Foundation for support for this research. Funds for the purchase of the X-ray equipment were made available from NSF Grant CHE-85-14495.

Supplementary Material Available: Tables of crystal data, final fractional coordinates, calculated hydrogen positions, bond distances and angles, and thermal parameters and a ball and stick drawing of **3** (13 pages); table of observed and calculated structure factor amplitudes (18 pages). Ordering information is given on any current masthead page.

Tetranuclear Organooxotin Cage Compounds Formed with Phosphate and Phosphonate Ligands.[1] A New Class of Organotin Clusters

K. C. Kumara Swamy, Charles G. Schmid,[2] Roberta O. Day, and Robert R. Holmes*

Contribution from the Department of Chemistry, University of Massachusetts, Amherst, Massachusetts 01003. *Received May 24, 1989*

Abstract: The hydrolysis of methyltin tris(diphenyl phosphate) in ether–methyl cyanide solution yielded a new tetranuclear methyltin cluster, $[Me_2Sn_2(OH)(O_2P(OPh)_2)_3(O_3POPh)]_2$ (**1**). Related derivatives resulted from the condensation reaction of phosphonic acids with *n*-butylstannonic acid in an acetone solution at room temperature, $[R'_2Sn_2O(O_2P(OH)R)_4]_2$: R′ = *n*-Bu, R = *t*-Bu (**2**); R′ = *n*-Bu, R = Et (**3**). Also **4** was synthesized (R′ = Me, R = *t*-Bu). X-ray analysis reveals related cage structures for **1** and **2**. Both contain Sn(IV) in a hexacoordinated environment in which the tin atoms are bridged by oxygen or hydroxyl species in addition to bridges by phosphate or phosphonate groups. ^1H, ^{31}P, and ^{119}Sn NMR data indicate retention of the solid-state structures in solution. The structural relation between possible cage formulations for **1** and **2** and related tetranuclear crown clusters is described. The crown formulations may be considered hydrolysis products of the cage derivatives. Hydrogen bonding aids in the formation of the cage skeletal arrangement, yielding a pocket potentially useful in clathration. **1** crystallizes in the triclinic space group $P\bar{1}$ with a = 13.100 (4) Å, b = 14.372 (4) Å, c = 14.958 (5) Å, α = 65.27 (2)°, β = 74.17 (3)°, γ = 87.99 (2)°, and Z = 1. **2** crystallizes in the triclinic space group $P\bar{1}$ with a = 12.037 (4) Å, b = 12.712 (2) Å, c = 14.771 (3) Å, α = 98.90 (2)°, β = 104.89 (2)°, γ = 107.41 (2)°, and Z = 1. The final conventional unweighted residuals are 0.024 (**1**) and 0.050 (**2**).

We have uncovered a rich cluster chemistry describing a variety of new structural forms for monoorganooxotin compounds containing ligands that result from the use of phosphorus-based acids.[1b,3] Thio derivatives also have been prepared that show interesting and logical structural variations.[3-5] Thus far, the tin nuclearities in these derivatives range from 2 to 7. Included among the geometrical frameworks are prismanes or drums,[6] cubes,[7,8] oxygen-capped clusters[6,8,9] and related sulfur-capped derivatives,[3-5] butterfly formations,[8] crowns,[1b] double cubes,[4] and extended clusters.[1b]

A principal reaction leading to their formation has been the condensation of an organostannoic acid with either a phosphinic, phosphonic, or phosphoric acid. Other reactions start with a previously formed cluster unit, which is then treated with a phosphorus-based acid. Both of these preparative methods are employed here and lead to the novel tetranuclear clusters, $[Me_2Sn_2(OH)(O_2P(OPh)_2)_3(O_3POPh)]_2$ (**1**) and $[(n\text{-}Bu)_2Sn_2O(O_2P(OH)\text{-}t\text{-}Bu)_4]_2$ (**2**), which represent yet a new structural class that may be described as "cage" formulations. Compared to previously reported cluster units, they are most closely related to the "crown" types.[1b] However, they present a unique feature in that each cage contains a flexible cavity potentially useful in clathration reactions. Reported in this paper are their syntheses, their X-ray structures, and a study of their ^1H, ^{119}Sn, and ^{31}P NMR solution-state spectra.

Experimental Section

Chemicals were obtained from Aldrich, Fisher Scientific, and Alfa and used without further purification. Methylstannonic acid was prepared according to the procedure given by Lambourne.[10] *n*-Butylstannonic acid was a gift from the Koriyama Kasei Co., Ltd., and was purified by using excess KOH in $CHCl_3$ to remove a small amount of *n*-$BuSn(OH)Cl_2$ and/or *n*-$BuSn(OH)_2Cl$ suspected[11] as a contaminant. Solvents used were of HPLC grade (Fisher). Further purification was done according to standard procedures.[12]

(1) (a) Organotin Clusters. 6. (b) Kumara Swamy, K. C.; Schmid C. G.; Day, R. O.; Holmes, R. R. *J. Am. Chem. Soc.* **1988**, *110*, 7067.
(2) This work represents in part a portion of: Schmid, C. G. Ph.D. Thesis, University of Massachusetts, Amherst, MA, 1989.
(3) Holmes, R. R. *Acc. Chem. Res.* **1989**, *22*, 190.
(4) (a) Kumara Swamy, K. C.; Day, R. O.; Holmes, R. R. *J. Am. Chem. Soc.* **1988**, *110*, 7543. (b) Day, R. O.; Kumara Swamy, K. C.; Schmid, C. G.; Holmes, R. R. *Phosphorus, Sulfur and Silicon* **1989**, *41*, 458.
(5) Schmid, C. G.; Day, R. O.; Holmes, R. R. *Phosphorus, Sulfur and Silicon* **1989**, *41*, 69.
(6) Day, R. O.; Chandrasekhar, V.; Kumara Swamy, K. C.; Holmes, J. M.; Burton, S. D.; Holmes, R. R. *Inorg. Chem.* **1988**, *27*, 2887.
(7) Kumara Swamy, K. C.; Day, R. O.; Holmes, R. R. *J. Am. Chem. Soc.* **1987**, *109*, 5546.
(8) Holmes, R. R.; Kumara Swamy, K. C.; Schmid, C. G.; Day, R. O. *J. Am. Chem. Soc.* **1988**, *110*, 7060.
(9) Day, R. O.; Holmes, J. M.; Chandrasekhar, V.; Holmes, R. R. *J. Am. Chem. Soc.* **1987**, *109*, 940.
(10) Lambourne, H. *J. Chem. Soc.* **1922**, *121* (2), 2533.
(11) Chandrasekhar, V.; Schmid, C. G.; Burton, S. D.; Holmes, J. M.; Day, R. O.; Holmes, R. R. *Inorg. Chem.* **1987**, *26*, 1050.
(12) Vogel, A. I. *Textbook of Practical Organic Chemistry*; Longman: London, 1978.

0002-7863/90/1512-223$02.50/0

^1H, ^{31}P, and ^{119}Sn NMR spectra (proton decoupled) were recorded on a Varian XL-300 FT/NMR spectrometer equipped with a multinuclear broad-band probe and operated at 300, 121.4, and 11.862 MHz, respectively. Resonances are referenced vs tetramethylsilane (^1H), tetramethyltin (external standard, ^{119}Sn), and 85% orthophosphoric acid (external standard, ^{31}P).

Preparation of Methyltin Tris(diphenyl phosphate), $MeSn(O_2P(OPh)_2)_3$. A mixture of hexameric methyloxotin acetate[6] (1.56 g, 1.25 mmol) and diphenylphosphoric acid (5.67 g, 22.66 mmol) was heated under reflux for 5 h with the azeotropic removal of water and acetic acid. The residual solvent was distilled at atmospheric pressure to yield the title compound as an oil: yield 6.6 g, ca. 100%; ^1H NMR ($CDCl_3$, ppm) 6.60–7.40 (br, aromatic), 0.20–0.90 (br, CH_3); ^{31}P NMR ($CDCl_3$, ppm) −10.85; ^{119}Sn NMR ($CDCl_3$, ppm) −648.5 (br). Anal. Calcd for $C_{37}H_{33}O_{12}P_3Sn$: C, 50.42; H, 3.75. Found: C, 49.65; H, 3.83.

Preparation of the Cage Cluster $[Me_2Sn_2(OH)(O_2P(OPh)_2)_3(O_3POPh)]_2$ (1). Methyltin tris(diphenyl phosphate) (3.6 g, 4.1 mmol) was dissolved in a mixture of diethyl ether (50 mL) and acetonitrile (80 mL). Water (0.5 g, 27.8 mmol) was added to the solution. Slow evaporation of the solvent at 20 °C yielded crystals of **1** sparingly soluble in chloroform: mp 205–210 °C; yield 1.0 g, 40.7%; ^1H NMR ($CDCl_3$, ppm) 6.80–7.40 (br, aromatic), 0.58 (br, CH_3, $^2J(Sn–C–H) \approx 146$ Hz), 0.22 (br, CH_3, $^2J(Sn–C–H) \approx 145$ Hz). The position of O*H* could not be ascertained with certainty. ^{31}P NMR ($CDCl_3$ + MeOH, ppm) −12.61 ($P(OPh)$, $^2J(Sn–O–P) = 240.9$ Hz), −17.04 ($P(OPh)_2$, $^2J(Sn–O–P) = 177.4$ Hz), −17.80 ($P(OPh)_2$, $^2J(Sn–O–P) = 228$ Hz), −23.94 ($P(OPh)_2$, $^2J(Sn–O–P) = 242.9$ Hz); ^{119}Sn NMR ($CDCl_3$ + MeOH, ppm) −602.0 (m). Anal. Calcd for $C_{88}H_{84}O_{34}P_8Sn_4$: C, 43.88; H, 3.50. Found: C, 43.84; H, 3.70. Crystals suitable for X-ray were grown from a mixture of dichloromethane and hexane.

Preparation of the Cage Cluster $[(n\text{-}Bu)_2Sn_2O(O_2P(OH)\text{-}t\text{-}Bu)_4]_2$ (2). *tert*-Butylphosphonic acid (0.60 g, 4.3 mmol) was dissolved in acetone (20 mL). *n*-Butylstannonic acid (0.47 g of 95% material, 2.1 mmol) was added. The light tan solution was filtered and evaporated overnight in the open air. Long, rectangular crystals remained. At 280 °C slight browning occurred. On further heating to 370 °C, the brown increased in intensity but no melting took place. The crystalline form was retained with no visible wetting: yield 0.69 g (71% based on stannonic acid); ^1H NMR ($CDCl_3$, ppm) 4.49 (s, with $^{117/119}Sn$ satellites, bridging OH groups, 1 H), 1.65 (m), 1.37 (m), 1.26 (m, methylene protons of *n*-Bu group, 12 H), 1.15 (d), 1.10 (d, two types of *t*-Bu group protons, 18 H each), 0.88 (t, Me protons of *n*-Bu group, 6 H); ^{119}Sn NMR ($CDCl_3$, ppm) −630.4 (tt, $^2J(Sn–O–P) = 239.2$, 286.5 Hz); ^{31}P NMR ($CDCl_3$, ppm) 30.1 (s, with $^{117/119}Sn$ satellites, 228.7, 239.1 Hz), 21.4 (s, with $^{117/119}Sn$ satellites, 274.1, 286.1 Hz). Anal. Calcd for $C_{48}H_{116}O_{26}Sn_4P_8$: C, 31.47; H, 6.40. Found: C, 31.49; H, 6.90.

Preparation of the Cage Cluster $[(n\text{-}Bu)_2Sn_2O(O_2P(OH)Et)_4]_2$ (3). Ethylphosphonic acid (0.54 g of 98%, 4.9 mmol) was dissolved in acetone (30 mL). *n*-Butylstannonic acid (0.53 g of 95% material, 2.4 mmol) was added. Chloroform (10 mL) was also added. This solution was filtered and evaporated. A white powder was obtained. The behavior on heating over the temperature range 280–370 °C was similar to that of **2**. Discoloration occurred with no loss of form: yield 0.86 g (90%); ^{119}Sn NMR ($CDCl_3$, ppm) −624.1 (tt, $^2J(Sn–O–P) = 223.5$, 236.4 Hz); ^{31}P NMR ($CDCl_3$, ppm) 27.6 (s, with $^{117/119}Sn$ satellites, 212.5, 222.6 Hz), 20.1 (s, with $^{117/119}Sn$ satellites, 226.4, 235.9 Hz). Anal. Calcd for $C_{32}H_{84}O_{26}Sn_4P_8$: C, 23.91; H, 5.28. Found: C, 24.04; H, 5.16.

Preparation of the Cage Cluster $[Me_2Sn_2O(O_2P(OH)\text{-}t\text{-}Bu)_4]_2$ (4). A mixture of dimeric bis(methyloxotin isobutyrate)methyltin triisobutyrate[13] (1.0 g, 0.72 mmol) and *tert*-butylphosphonic acid (1.19 g, 8.61 mmol) was dissolved in acetone (40 mL) and set aside. After ca. 18 h, a microcrystalline precipitate was obtained: mp > 370 °C; yield 1.4 g, ca. 84.3%, sparingly soluble in chloroform). NMR spectra showed it to be mostly compound **4**: >90%; ^1H NMR ($CDCl_3$, ppm) 4.60 (O*H*), 1.15 (d, $t\text{-}C_4H_9$, $^3J(P–H) = 6.8$ Hz), 1.11 (d, $t\text{-}C_4H_9$, $^3J(P–H) = 6.1$ Hz), 0.54 (CH_3Sn, $^2J(Sn–H) = 140.2$ Hz); 1.48 (d, $^3J(P–H) = 6.3$ Hz, impurity); ^{31}P NMR ($CDCl_3$, ppm) 29.81 ($^2J(Sn–O–P) = 215.0$ Hz), 21.94 ($^2J(Sn–O–P) = 229.0$ Hz); ^{119}Sn NMR ($CDCl_3$, ppm) −603.5 (m). Anal. Calcd for $C_{36}H_{92}O_{26}P_4Sn_4$: C, 28.08; H, 6.00. Found: C, 26.63; H, 5.64.

X-ray Studies. All X-ray crystallographic studies were done with an Enraf-Nonius CAD4 diffractometer and graphite-monochromated molybdenum radiation ($\lambda K\bar{\alpha} = 0.71073$ Å) at an ambient temperature of 23 ± 2 °C. Details of the experimental procedures have been described previously.[14]

Crystals were mounted in thin-walled glass capillaries, which were sealed as a precaution against moisture sensitivity. Data were collected with the use of the θ–2θ scan mode ($3° \le 2\theta_{Mo K\bar{\alpha}} \le 43°$; $+h,\pm k,\pm l$). Empirical absorption corrections based on ψ scans were applied (relative transmission factors on *I* from 0.909 to 1.00 for **1** and from 0.870 to 1.00 for **2**).

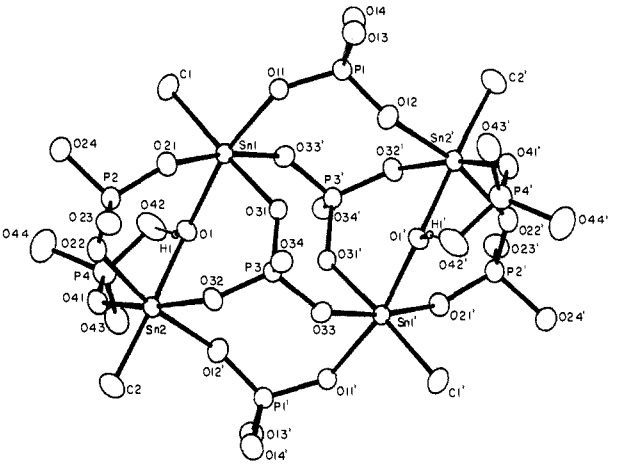

Figure 1. ORTEP plot of $[Me_2Sn_2(OH)(O_2P(OPh)_2)_3(O_3POPh)]_2$ (**1**) with thermal ellipsoids at the 30% probability level. Hydrogen atoms except for H1 and phenyl group carbon atoms (C11–C16 through C71–C76) are omitted for clarity. The hydrogen bonds are shown as narrow lines. Primed atoms are inversion related ($-x, -y, -z$).

The structures were solved by use of Patterson and difference Fourier techniques and were refined by full-matrix least squares.[15] All computations were performed on a Microvax II computer using the Enraf-Nonius SPD system of programs.

X-ray Study for $[Me_2Sn_2(OH)(O_2P(OPh)_2)_3(O_3POPh)]_2$ (1). Colorless crystals of **1** are thin laths and plates. The crystal used for the X-ray study was cut to dimensions of 0.10 × 0.20 × 0.38 mm.

Crystal data: $(C_{44}H_{42}O_{17}P_4Sn_2)_2$; triclinic space group $P\bar{1}$ [C_i^1–No. 2];[16] $a = 13.100$ (4), $b = 14.372$ (4), $c = 14.958$ (5) Å; $\alpha = 65.27$ (2), $\beta = 74.17$ (3), $\gamma = 87.99$ (2)°; $Z = 1$; $\mu_{Mo K\bar{\alpha}} = 12.178$ cm^{-1}. A total of 5617 independent reflections was measured.

The 67 independent non-hydrogen atoms were refined anisotropically. The 35 independent aromatic hydrogen atoms (idealized positions) and the six independent methyl hydrogen atoms (regularized difference Fourier positions) were included in the refinement as fixed isotropic scatterers. The independent H1, of the bridging hydroxyl group, appeared as the most prominent feature on a difference Fourier synthesis and was also included in the refinement as a fixed isotropic scatterer. The final agreement factors[17] were $R = 0.024$ and $R_w = 0.033$ for the 4696 reflections having $I \ge 3\sigma_I$.

X-ray Study for $[(n\text{-}Bu)_2Sn_2O(O_2P(OH)\text{-}t\text{-}Bu)_4]_2$ (2). The crystal used for the X-ray study was cut from a colorless thin lath and had dimensions of 0.23 × 0.35 × 0.49 mm.

Crystal data: $(C_{24}H_{58}O_{13}P_4Sn_2)_2$; triclinic space group $P\bar{1}$; $a = 12.037$ (4) Å, $b = 12.712$ (2) Å, $c = 14.771$ (3) Å; $\alpha = 98.90$ (2)°, $\beta = 104.89$ (2)°, $\gamma = 107.41$ (2)°; $Z = 1$; $\mu_{Mo K\bar{\alpha}} = 14.472$ cm^{-1}. A total of 4608 independent reflections was measured.

The 43 independent non-hydrogen atoms were refined anisotropically. The hydrogen atoms of the independent *t*-Bu groups and the methylene hydrogen atoms of the independent *n*-Bu groups (48 H atoms) were included in the refinement in idealized positions as fixed isotropic scatterers. The six independent hydrogen atoms of the terminal carbon atoms of the *n*-Bu groups were omitted from the refinement. A difference Fourier synthesis showed electron density in the vicinity of both the hydroxyl oxygen atoms bonded to phosphorus and the bridging oxygen atom, but as this density was at the noise level, it was judged to be unreliable and the four independent hydrogen atoms in question were omitted from the refinement. The final agreement factors[17] were $R = 0.050$ and $R_w = 0.074$ for the 3921 reflections having $I \ge 3\sigma_I$.

Results

The molecular geometry of the framework of **1** is shown in the ORTEP plot of Figure 1. Selected bond lengths and angles are given in Table I. The corresponding information for **2** is given in Figure 2 and in Table II. Atomic coordinates and anisotropic

(13) Nadim, H. M.S. Thesis, University of Massachusetts, Amherst, MA, 1988.

(14) Sau, A. C.; Day, R. O.; Holmes, R. R. *Inorg. Chem.* **1981**, *20*, 3076.

(15) The function minimized was $\sum w(|F_o| - |F_c|)^2$, where $w^{1/2} = 2F_oLp/\sigma_I$.

(16) *International Tables for X-ray Crystallography*; Kynoch: Birmingham, England, 1969; Vol. I, p 75.

(17) $R = \sum||F_o| - |F_c||/\sum|F_o|$ and $R_w = [\sum w(|F_o| - |F_c|)^2/\sum w|F_o|^2]^{1/2}$.

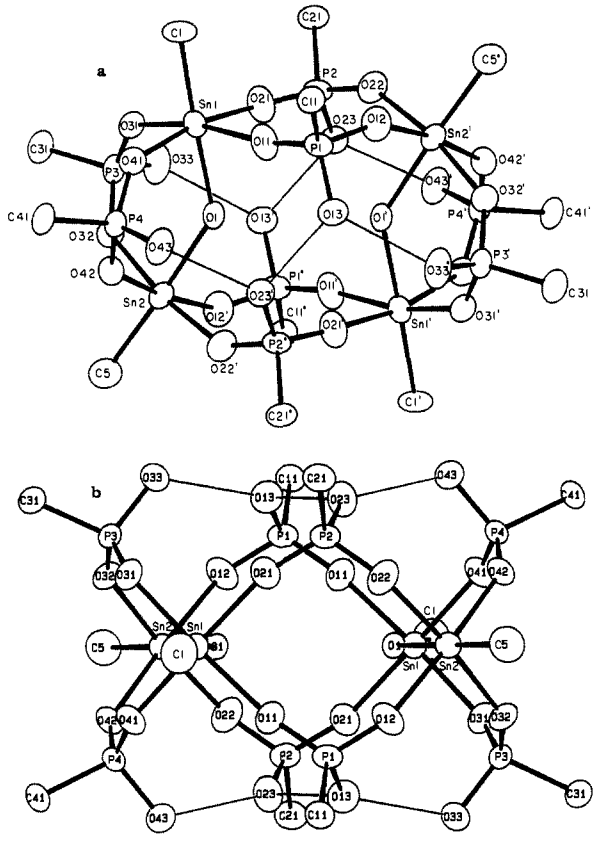

Figure 2. (a) ORTEP plot of $[n\text{-}Bu_2Sn_2O(O_2P(OH)\text{-}t\text{-}Bu)_4]_2$ (**2**) with thermal ellipsoids at the 30% probability level. Hydrogen atoms, pendant carbon atoms of the *n*-Bu groups (C2–C4 and C6–C8), and pendant carbon atoms of the *t*-Bu groups (C12–C14 bonded to C11, C22–C24 bonded to C21, etc.) are omitted for clarity. Hydrogen-bonding interactions are indicated by the narrow lines. Primed atoms are inversion related ($-x, -y, -z$). (b) ORTEP plot of **2** similar to (a) but rotated 90° with a view perpendicular to the pseudo-2-fold axis.

thermal parameters, complete tabulations of bond lengths and angles, and hydrogen atom parameters are provided as supplementary material.

Discussion

Syntheses. The use of three different preparative routes has led to the structurally similar tetranuclear organotin clusters **1–4**. The methyltin derivative **1** resulted from an unique hydrolysis reaction of methyltin tris(diphenyl phosphate) in an ether–acetonitrile solution (eq 1), whereas the others, **2–4**, were obtained

$$4MeSn(O_2P(OPh)_2)_3 + 4H_2O \rightarrow [Me_2Sn_2(OH)\text{-}(O_2P(OPh)_2)_3(O_3P(OPh))]_2 + 2PhOH + 4(PhO)_2PO_2H \quad (1)$$

by condensation reactions. In the case of the synthesis of **2** and **3**, *n*-butylstannonic acid was reacted with the respective phosphonic acid in acetone solution (eq 2), while the formation of **4** resulted

$$4\,n\text{-}BuSn(O)OH + 8RPO(OH)_2 \rightarrow [n\text{-}Bu_2Sn_2O(O_2P(OH)R)_4]_2 + 6H_2O \quad (2)$$

$$R = t\text{-}Bu\ (\mathbf{2});\ Et\ (\mathbf{3})$$

from a displacement reaction of a carboxylate cluster unit with *tert*-butylphosphonic acid in acetone solution (eq 3). All of these syntheses were conducted at ambient temperature.

$$2[(MeSn(O)O_2CCHMe_2)_2MeSn(O_2CCHMe_2)_3]_2 + 24\,t\text{-}BuPO(OH)_2 \rightarrow 3[Me_2Sn_2O(O_2P(OH)\text{-}t\text{-}Bu)_4]_2 + 20Me_2C(H)CO_2H + 2H_2O \quad (3)$$

Of the previous tin clusters that have been described, both **1** and **2** bear some resemblance to the tetranuclear crown clusters[1b] $[(n\text{-}BuSn(O)O_2P(t\text{-}Bu)_2)(n\text{-}BuSn(OH)_2O_2P(t\text{-}Bu)_2)]_2[H][O_2P(t\text{-}Bu)_2]$ (crown A) and $[(MeSn(O)O_2P(t\text{-}Bu)_2)(MeSn(OH)(OMe)O_2P(t\text{-}Bu)_2)]_2[H][O_2P(t\text{-}Bu)_2]\cdot 4MeOH\cdot 2H_2O$ (crown B). A comparison of the cationic portion of the crown with the cage **1** is shown in schematic form (Chart I). The crown clusters result from reactions of phosphinic acids with other cluster units as starting materials, e.g., a drum (prismane) to prepare crown A and a mixed-drum derivative to prepare crown B, in addition to direct condensation of the stannonic and phosphinic acids, the latter also giving crown A.[1b] For all of these methods, the reaction mixtures were heated and relatively low yields of the crowns resulted from the mixtures of products.[1b]

One can write an equation expressing the relationship between the crown formulation and the presently described cages. Specifically for **1**, eq 4 results. However, the reaction is not probable

$$[R'_2Sn_2(OH)(O_2PR_2)_3(O_3PR)]_2 + 4H_2O \rightarrow \underset{\text{cage } \mathbf{1}}{} [(R'Sn(O)O_2PR_2)(R'Sn(OH)_2O_2PR_2)]_2[H][O_2PR_2] + \underset{\text{crown}}{} R_2P(O)(OH) + 2RPO(OH)_2 \quad (4)$$

$$R' = Me,\ R = OPh$$

since the crown formulations contain phosphinate ligands, whereas the cages contain phosphonate or phosphate ligands. Most likely, the increased ligating properties of the latter types of acids are

Table I. Selected Distances (Å) and Angles (deg) for $[Me_2Sn_2(OH)(O_2P(OPh)_2)_3(O_3POPh)]_2$ (**1**)[a]

atom 1–atom 2	dist	atom 1–atom 2	dist
Sn1–O1	2.082 (2)	O22–P2	1.490 (2)
Sn1–O11	2.118 (2)	O23–P2	1.573 (3)
Sn1–O21	2.157 (3)	O23–C31	1.401 (4)
Sn1–O31	2.027 (3)	O24–P2	1.568 (3)
Sn1–O33′	2.075 (3)	O24–C41	1.416 (6)
Sn1–Cl	2.108 (5)	O31–P3	1.513 (2)
Sn2–O1	2.037 (2)	O32–P3	1.512 (3)
Sn2–O12′	2.126 (3)	O33–P3	1.509 (3)
Sn2–O22	2.143 (3)	O34–P3	1.583 (2)
Sn2–O32	2.081 (2)	O34–C51	1.407 (5)
Sn2–O41	2.115 (3)	O41–P4	1.517 (3)
Sn2–C2	2.104 (4)	O42–P4	1.475 (3)
O11–P1	1.490 (3)	O43–P4	1.578 (3)
O12–P1	1.479 (3)	O43–C61	1.400 (5)
O13–P1	1.577 (2)	O44–P4	1.572 (4)
O13–C11	1.409 (5)	O44–C71	1.394 (6)
O14–P1	1.574 (3)	H1–O1	0.951 (2)
O14–C21	1.398 (6)	H1–O42	1.644 (3)
O21–P2	1.490 (3)		

atom 1–atom 2–atom 3	angle	atom 1–atom 2–atom 3	angle
O1–Sn1–O11	166.4 (1)	O22–Sn2–O32	85.4 (1)
O1–Sn1–O21	88.64 (9)	O22–Sn2–O41	94.4 (1)
O1–Sn1–O31	86.86 (9)	O22–Sn2–C2	94.1 (2)
O1–Sn1–O33′	86.81 (9)	O32–Sn2–O41	169.3 (1)
O1–Sn1–Cl	100.1 (1)	O32–Sn2–C2	95.6 (1)
O11–Sn1–O21	94.08 (9)	O41–Sn2–C2	95.1 (1)
O11–Sn1–O31	80.27 (9)	Sn1–O1–Sn2	136.6 (1)
O11–Sn1–O33′	88.67 (9)	Sn1–O11–P1	138.8 (1)
O11–Sn1–Cl	93.1 (1)	Sn2′–O12–P1	149.3 (2)
O21–Sn1–O31	83.4 (1)	P1–O13–C11	123.3 (2)
O21–Sn1–O33′	171.3 (1)	P1–O14–C21	125.3 (3)
O21–Sn1–Cl	91.4 (1)	Sn1–O21–P2	133.9 (1)
O31–Sn1–O33′	88.9 (1)	Sn2–O22–P2	132.9 (2)
O31–Sn1–Cl	171.3 (1)	P2–O23–C31	123.2 (3)
O33–Sn1–Cl	96.7 (1)	P2–O24–C41	127.0 (2)
O1–Sn2–O12′	85.3 (1)	Sn1–O31–P3	134.8 (2)
O1–Sn2–O22	83.9 (1)	Sn2–O32–P3	136.5 (2)
O1–Sn2–O32	85.20 (9)	Sn1′–O33–P3	137.0 (2)
O1–Sn2–O41	84.1 (1)	P3–O34–C51	120.8 (2)
O1–Sn2–C2	177.8 (2)	Sn2–O41–P4	133.1 (2)
O12′–Sn2–O22	168.22 (9)	P4–O43–C61	121.7 (3)
O12′–Sn2–O32	88.9 (1)	P4–O44–C71	128.4 (3)
O12′–Sn2–O41	89.3 (1)	O1–H1–O42	167.7 (2)
O12′–Sn2–C2	96.7 (2)		

[a] Estimated standard deviations in parentheses. The atom-labeling scheme is shown in Figure 1.

Table II. Selected Distances (Å) and Angles (deg) for $[(n\text{-Bu})_2Sn_2O(O_2P(OH)\text{-}t\text{-Bu})_4]_2$ (**2**)[a]

atom 1–atom 2	dist	atom 1–atom 2	dist
Sn1–O1	2.099 (6)	O11–P1	1.458 (7)
Sn1–O11	2.110 (7)	O12–P1	1.515 (6)
Sn1–O21	2.097 (6)	O13–P1	1.563 (8)
Sn1–O31	2.085 (6)	O21–P2	1.458 (6)
Sn1–O41	2.079 (5)	O22–P2	1.512 (7)
Sn1–C1	2.12 (1)	O23–P2	1.575 (6)
Sn2–O1	2.153 (6)	O31–P3	1.515 (6)
Sn2–O12′	2.075 (6)	O32–P3	1.498 (7)
Sn2–O22′	2.069 (8)	O33–P3	1.561 (6)
Sn2–O32	2.089 (6)	O41–P4	1.510 (7)
Sn2–O42	2.089 (5)	O42–P4	1.520 (6)
Sn2–C5	2.14 (1)	O43–P4	1.559 (8)
O13–O23′	2.424 (9)	O13–O33′	2.616 (9)
O23–O43′	2.550 (7)		

atom 1–atom 2–atom 3	angle	atom 1–atom 2–atom 3	angle
O1–Sn1–O11	81.6 (3)	O12′–Sn2–O22′	88.5 (3)
O1–Sn1–O21	83.5 (3)	O12′–Sn2–O32	88.8 (2)
O1–Sn1–O31	85.8 (2)	O12′–Sn2–O42	171.9 (3)
O1–Sn1–O41	85.2 (2)	O12′–Sn2–C5	94.8 (3)
O1–Sn1–C1	175.9 (4)	O22′–Sn2–O32	171.0 (2)
O11–Sn1–O21	89.6 (3)	O22′–Sn2–O42	91.0 (2)
O11–Sn1–O31	167.3 (3)	O22′–Sn2–C5	94.6 (4)
O11–Sn1–O41	89.0 (2)	O32–Sn2–O42	90.4 (2)
O11–Sn1–C1	94.4 (4)	O32–Sn2–C5	94.2 (4)
O21–Sn1–O31	87.6 (2)	O42–Sn2–C5	93.3 (3)
O21–Sn1–O41	168.7 (3)	Sn1–O1–Sn2	136.4 (2)
O21–Sn1–C1	97.6 (4)	Sn1–O11–P1	169.1 (5)
O31–Sn1–O41	91.3 (2)	Sn2′–O12–P1	144.8 (5)
O31–Sn1–C1	98.2 (4)	Sn1–O21–P2	164.4 (5)
O41–Sn1–C1	93.7 (3)	Sn2′–O22–P2	145.6 (5)
O1–Sn2–O12′	87.6 (2)	Sn1–O31–P3	136.2 (4)
O1–Sn2–O22′	87.4 (3)	Sn2–O32–P3	138.5 (3)
O1–Sn2–O32	83.9 (2)	Sn1–O41–P4	137.0 (3)
O1–Sn2–O42	84.4 (2)	Sn2–O42–P4	137.1 (3)
O1–Sn2–C5	177.0 (3)		

[a] Estimated standard deviations in parentheses. The atom-labeling scheme is shown in Figure 2.

responsible for the main structural differences between the two classes of compounds.

NMR Spectra. The ^{119}Sn NMR spectrum for the methyl cage **1** exhibits a multiplet pattern at −602.0 ppm (in a $CDCl_3$–MeOH mixture). The ^{31}P spectrum contains four resonances with tin satellites apparent for each. Assuming the ^{119}Sn multiplet contains signals from two kinds of tin atoms, these patterns are consistent with the schematic diagram illustrated above showing two pairs of tin atoms in solution and four pairs of phosphate ligands.

The patterns for **2**–**4**, which contain phosphonate ligands, differ from **1** in that only two kinds of phosphonate ligands are indicated. This is consistent with the presence of phosphonates acting as bidentate ligands as is somewhat apparent in Figure 2 compared to the phosphate ligand in **1**, which bonds in uni-, bi-, and tridentate fashion. As a consequence of the lesser complexity of ligand bonding, the ^{119}Sn pattern is greatly resolved, e.g., for **2** shown in Figure 3a. The two pairs of phosphonates linked to each tin atom yield a triplet of triplets with a ^{119}Sn shift of −630.4 ppm ($CDCl_3$). This is very similar to the ^{119}Sn pattern for the ethyl phosphonate cluster **3**, ^{119}Sn shift at −624.1 ppm ($CDCl_3$), and this supports a similar solution-state structure as indicated for **2**. The methyl derivative **4**, like **1**, has a lower ^{119}Sn chemical shift, −603.5 ($CDCl_3$), than found for the *n*-butyl derivatives **2** and **3**. Figure 3b portrays the ^{31}P spectrum for **2**, which is representative of that for **3** and **4**. The two resonances that are seen with tin satellites correspond to the presence of two kinds of phosphonate groups bridging pairs of symmetry-equivalent tin atoms. It is concluded that the solid-state structures found for the cage clusters **1** and **2** are essentially retained in solution. Further, the similarity in NMR patterns and chemical shifts suggests that the solution-state structures of **3** and **4** are closely related to **2**.

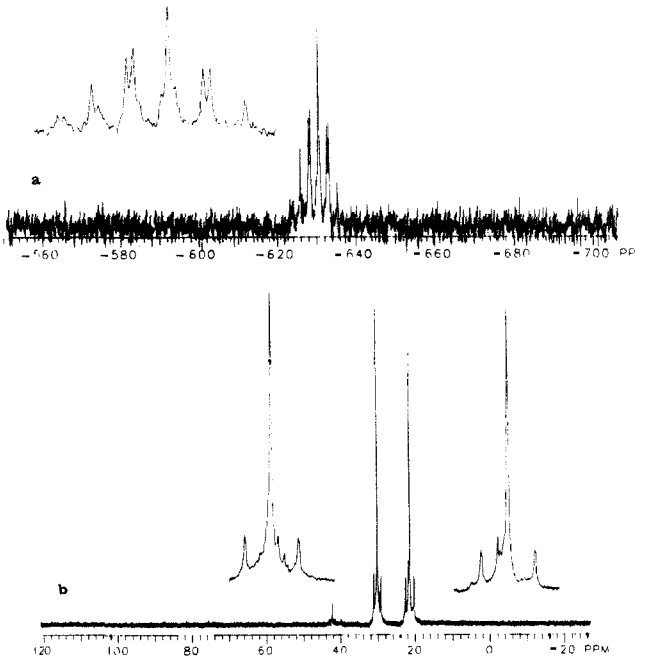

Figure 3. (a) ^{119}Sn NMR spectrum of the cage cluster **2** in $CDCl_3$ solution. (b) ^{31}P NMR spectrum of **2** in $CDCl_3$ solution.

Chart I

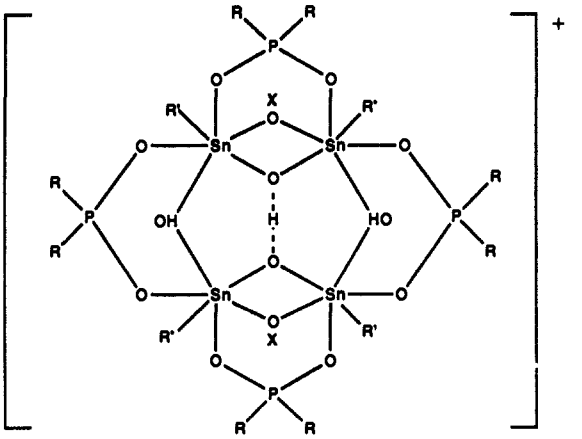

A: R′ = *n*-Bu, R = *t*-Bu, X = H
B: R′ = Me, R = *t*-Bu, X = Me

Crown

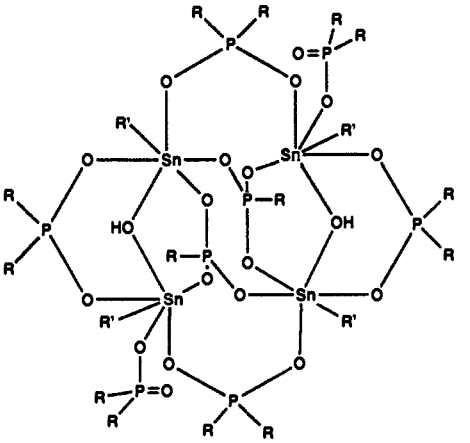

R′ = Me, R = OPh, Cage 1

The ^{119}Sn chemical shifts for the cage formulations are at the upper end of the chemical shift range found for other organotin

clusters formed from phosphorus ligands. This observation reflects a trend, indicating an increase in shielding as the ratio of phosphorus ligand to tin increases.

Cage compound **2** is very soluble in many organic solvents. This is in contrast to that observed for **1**, **3**, and **4** and suggests that the outer sheath of eight *tert*-butyl groups and four *n*-butyl groups that surround the tin–oxygen–phosphorus interior in **2** presents a lyophilic surface. The hydrogen-bonding scheme in the interior contributes to the formation of the cage-like structure and leads to a "pocket" with approximately 4 Å between the centers of the oxygen atoms. This cavity should be sufficiently flexible as a result of rearrangement of hydrogen bonding to host a variety of small molecules and ions.

Structural Details. Both structures have crystallographic C_i symmetry. For **1**, the idealized molecular symmetry is also C_i and thus there are two environments for the four tin atoms and four environments for the eight phosphorus atoms.

Phosphates P1 and P2 form symmetrical bridges between Sn1 and Sn2′ and between Sn1 and Sn2, respectively. Phosphate P4 is dangling, where the phosphoryl oxygen atom, O42, is the acceptor atom in a hydrogen bond with the hydroxyl group that also bridges Sn1 and Sn2. The aforementioned structural motifs have been previously observed.[1b,8] Phosphate P3 forms simultaneous symmetrical bridges between three tin atoms: Sn1 and Sn1′, Sn1 and Sn2, and Sn2 and Sn1′. This structural feature has not been observed previously.

In compound **2**, all of the tin centers are pairwise connected by two symmetrical phosphonate bridges forming a cyclic system. In addition, there are two oxygen (or hydroxide) bridges connecting pairs of tin atms. Although isomers are possible with respect to the orientation of the *t*-Bu group and the OH group at each phosphorus center, all of the phosphonate groups have the same disposition. For each bridging pair, the *t*-Bu groups are cis and directed away from the pseudo 2-fold axis (vide infra) that passes through the center of the molecule. This arrangement results in the formation of two zigzag chains of four oxygen atoms each, on opposite sides of the molecule, where the oxygen atoms of the chains are in hydrogen-bonding proximity (2.429 (9)–2.616 (9) Å). These hydrogen-bonding interactions cause the open cyclic system to be a cagelike structure, with the bridging oxygen atoms (O1 and O1′) in the interior of the cage.

In addition to crystallographic C_i symmetry, compound **2** has a noncrystallographic mirror plane that contains the four Sn atoms and the two bridging oxygen atoms and passes through the center of symmetry. Thus, the observed molecular symmetry in the solid state is C_{2h}, where the pseudo-2-fold axis is perpendicular to the pseudo mirror plane. In the absence of constraints imposed by the hydrogen bonds and packing effects in the solid, the highest idealized molecular symmetry would be D_{2h}, with the two additional mirror planes passing through P1, P2, P1′, and P2′ and P3, P4, P3′, and P4′, respectively. Thus, in solution, when the constraints imposed by static hydrogen bonds are relaxed, one type of tin and two types of phosphorus would be obtained.

For **2**, there must be eight hydrogen atoms bonded to oxygen atoms in order for electrical neutrality to be maintained. The X-ray study did not permit location of these hydrogen atoms, and the location of only six of the eight can be inferred from the non-hydrogen atom geometry. To account for the six hydrogen bonds, six of the hydrogen atoms must be bonded to six of the eight phosphonate group oxygen atoms. The remaining two hydrogen atoms could be similarly bound or could be bound to the bridging oxygen atoms O1 and O1′. Thus, **2** could be formulated either as $[(n\text{-Bu})_2Sn_2O(O_2P(OH)\text{-}t\text{-Bu})_4]_2$ with all eight of the hydrogen atoms as phosphonate –OH groups or as $[(n\text{-Bu})_2Sn_2(OH)(O_2P(OH)\text{-}t\text{-Bu})_3(O_3P\text{-}t\text{-Bu})]_2$ with OH groups bridging the tin centers. The latter formulation is strikingly like that of the structurally dissimilar $[Me_2Sn_2(OH)(O_2P(OPh)_2)_3(O_3POPh)]_2$, which perhaps argues against it. If **2** were hydroxo-bridged, this would leave P4 or P3′ and P4′ or P3 similarly structured as P3 (P3′) of **1**. As a consequence, one would expect these phosphate environments of **2** to tricoordinate to tin atoms and give a structure resembling **1** more closely than observed. This argument favors the oxo-bridged structure for **2**, schematically compared with **1** in Chart II. Comparison of Sn–O bond lengths

Chart II

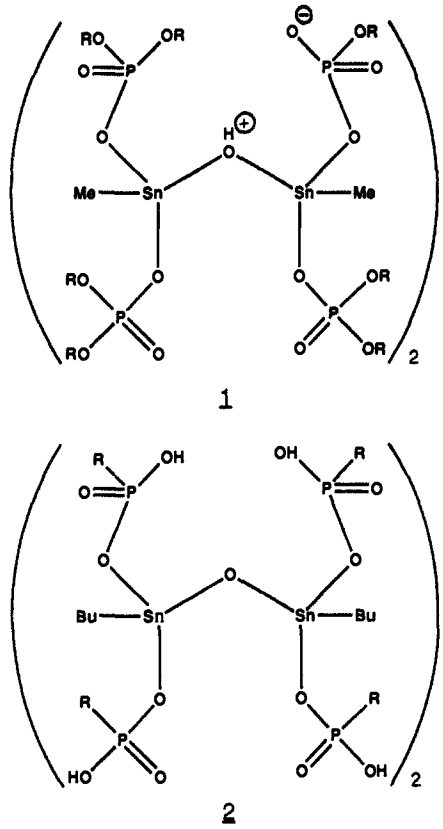

Chart III

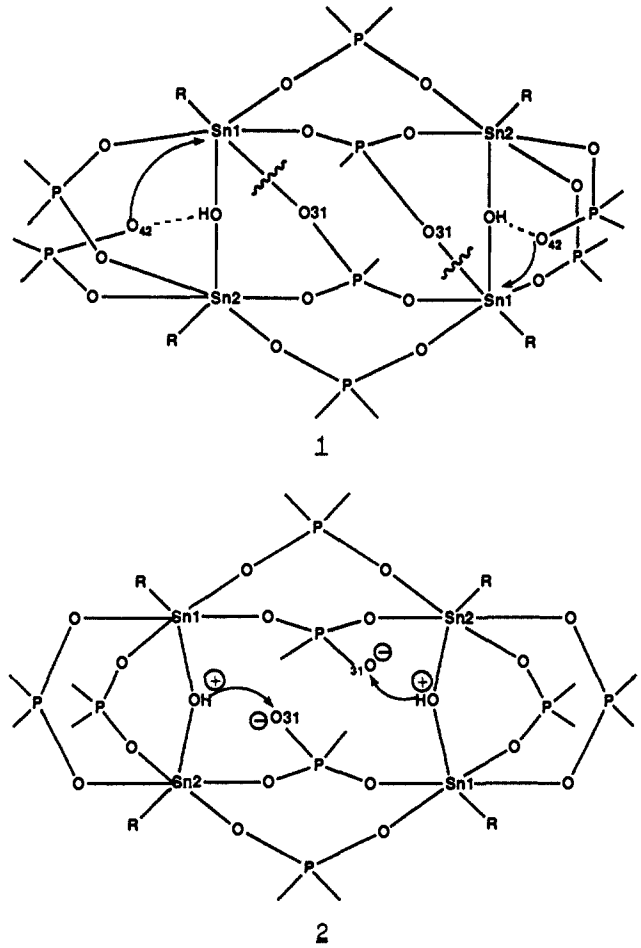

of **1** and **2** with other oxo- and hydroxo-bridged tin clusters[1b,6-9] does not assist in deciding between the two possibilities for **2**.

There is a close relationship between the apparently dissimilar frameworks indicated for **1** and **2**, which can be viewed, before assembly, as tautomers. The interconversion of the framework of **1** to the framework of **2** is illustrated in Chart III. On each side of the molecule of **1**, the hydrogen bond is broken followed by the formation of a bond between O42 and Sn1 with a simultaneous rupture of the bond between Sn1 and O31. The hydrogen atom of the bridging hydroxyl group could simultaneously be transferred to O31, leaving in **2** a bridging oxygen atom. However, it remains to uniquely establish the nature of these bridging positions in **2**.

Structural Analogies. Phosphate ligands appear in a unique arrangement in the cage cluster **1** coordinated to tin atoms in mono-, bi-, and tridentate fashion, whereas in **2** only bicoordination is observed. A complex, $(Me_2Sn)_3(PO_4)_2 \cdot 8H_2O$,[18] exhibiting hexacoordination around a Me_2Sn moiety, shows bi- and tetracoordination for phosphate ligands.

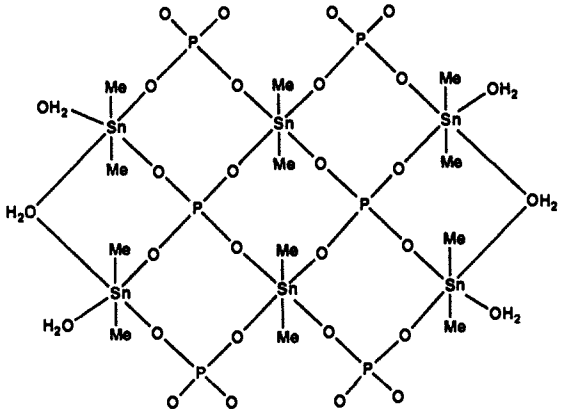

Structurally, more closely related to **1** is the aluminum phosphate, $[Al(PO_4)(HCl)(EtOH)_4]_4$,[19] made up of six eight-membered Al-O-P rings. The skeletal arrangement is shown:

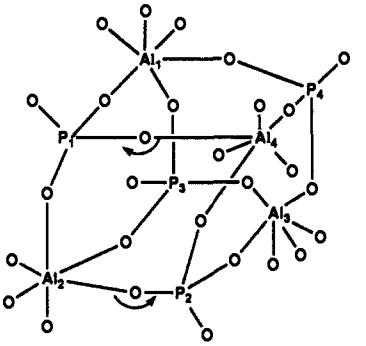

Cleavage of the Al_4-O(P_1) and Al_2-O(P_2) bonds and formation of hydroxide bridges, Al_1-O(H)-Al_4 and Al_2-O(H)-Al_3, lead to a similar framework representation that is found for **1**.

Acknowledgment. The support of this research by the National Science Foundation (Grants CHE-8504737 and CHE-8819152), the donors of the Petroleum Research Fund, administered by the American Chemical Society, and a Faculty Research Grant from the University of Massachusetts (to R.O.D.) is gratefully acknowledged.

Supplementary Material Available: Listings of atomic coordinates, anisotropic thermal parameters, additional bond lengths and angles, and hydrogen atom parameters (Tables S1-S4, respectively, for **1** and Tables S5-S8, respectively, for **2**) (22 pages); tables of calculated and observed structure factors (37 pages). Ordering information is given on any current masthead page.

(18) Ashmore, J. P.; Chivers, T.; Kerr, K. A.; Van Roude, J. H. G. *Inorg. Chem.* **1977**, *16*, 191.

(19) Cassidy, J. E.; Jarvis, J. A. J.; Rothon, R. N. *J. Chem. Soc., Dalton Trans.* **1975**, 1497.

Synthesis and Dynamic Behavior of (1,5)Cyclooctatetraenophanes. Effect of Distal Atom Bridging on Racemization Rates and Electrochemical Reducibility

Leo A. Paquette,* Michael P. Trova, Jihmei Luo, Amy E. Clough, and Larry B. Anderson

Contribution from the Department of Chemistry, The Ohio State University, Columbus, Ohio 43210. *Received March 3, 1989*

Abstract: The [5]-, [6]-, [8]-, and [10](1,5)cyclooctatetraenophanes as well as non-C_2-symmetric methyl homologues of these 1,5-bridged [8]annulenes have been prepared conveniently via a route that holds promise of considerable generality. The scheme consists of applying the Cook-Weiss procedure to a cyclic α-diketone, transforming the carbonyl groups of the product into a pair of olefinic sites (with or without attachment of the methyl substituent), preparation of the bracketed semibullvalene via nickel carbonyl promoted cyclization of the doubly allylic dibromide, and finally flash vacuum pyrolysis of the semibullvalene. Cyclic voltammetric studies performed on the title compounds have quantified not only the standard electron-donating capacity of the pendant alkyl groups, but also the consequences of nonbonded steric interactions associated with maintaining a bridged structure as the cyclooctatetraene ring flattens. Microscale preparation of the dianion of **5d** permitted measurement of its ^1H NMR spectrum. Whereas **5b-d** reacted with (-)-*endo*-bornyltriazolinedione, the methyl congeners **15** and **21** did not. Chromatographic separation of the urazole diastereomers derived from **5c** and **5d** proved possible. Whereas hydrolysis-oxidation of individual adducts provided access to optically active **5c**, **5d** was invariably already racemized upon isolation. Thus, the latter experiences very rapid conversion to its enantiomer. The activation parameters for racemization within **5c** were determined, and it is argued that these reflect exclusively the energetic costs of bond shifting within its [8]annulene core.

Interest in the conformational dynamics of molecules carrying polymethylene chains has persisted for almost 50 years for many reasons.[1] The successful resolution of **1** by Lüttringhaus,[2] of **2** by Cram and Allinger[3] and by Blomquist,[4] and of **3** by Gerlach

0002-7863/90/1512-228$01.50/0